MASSIVE-TRAINING ARTIFICIAL NEURAL NETWORKS FOR CAD FOR DETECTION OF POLYPS IN CT COLONOGRAPHY: FALSE-NEGATIVE CASES IN A LARGE MULTICENTER CLINICAL TRIAL

Kenji Suzuki, PhD, Mark Epstein, MS, Ivan Sheu, Ryan Kohlbrenner, BS
Don C. Rockey, MD, Abraham H. Dachman, MD*

Department of Radiology, The University of Chicago, Chicago, IL
* Department of Internal Medicine, The University of Texas Southwestern Medical Center, Dallas, TX

ABSTRACT

A major challenge in computer-aided detection (CAD) of polyps in CT colonography (CTC) is the detection of "difficult" polyps which radiologists are likely to miss. Our purpose was to develop massive-training artificial neural networks (MTANNs) for improving the performance of a CAD scheme on false-negative cases in a large multicenter clinical trial. We developed 3D MTANNs designed to differentiate between polyps and several types of non-polyps and tested on 14 polyps/masses that were actually "missed" by radiologists in the trial. Our initial CAD scheme detected 71.4% of "missed" polyps with 18.9 false positives (FPs) per case. The MTANNs removed 75% of the FPs without loss of any true positives; thus, the performance of our CAD scheme was improved to 4.8 FPs per case at the sensitivity of 71.4% of the polyps "missed" by radiologists.

Index Terms— computer-aided detection, virtual colonoscopy, missed lesions, false positive reduction, polyps

1. INTRODUCTION

Colorectal cancer is the second leading cause of cancer deaths in the U.S. CT colonography (CTC) is a relatively new technique for detecting colorectal neoplasms by use of a CT scan of the colon. The diagnostic performance of CTC in detecting polyps (i.e., precursors of cancer), however, remains uncertain [1-5] due to a propensity for perceptual errors [6]. Computer-aided detection (CAD) of polyps has the potential to overcome this difficulty with CTC [7, 8].

Summers et al. [9] developed a CAD scheme and they achieved a sensitivity of 64% with a FP rate of 6 per colon, based on a 20-patient database with 28 polyps. Yoshida et al. [8] reported their CAD scheme yielded a 89% by-polyp sensitivity with 2.5 FPs per patient, based on 9 patients with 18 polyps. Jerebko et al. [10] reported their CAD scheme yielded a sensitivity of 90% with 15.7 FPs per scan, based on 40 patients with a total of 39 polyps in 20 patients [10]. Paik et al. [11] reported their CAD scheme yielded a sensitivity of 100% with 7.0 FPs per data set based on eight patients that included seven polyps in four patients.

A major challenge in CAD development is the detection of "difficult" polyps which radiologists are likely to miss. None of the above studies used polyps "missed" by radiologists. Our purpose was to develop a CAD scheme incorporating 3D massive-training artificial neural networks (MTANNs) for the detection of polyps in CTC and to evaluate its performance on false-negative (FN) cases that radiologists actually "missed" in a large multicenter clinical trial [12, 13].

2. OUR CAD SCHEME WITH 3D MTANNS

2.1. An Initial Polyp-Detection Scheme

Our initial polyp-detection scheme consists of 1) colon segmentation based on CT value-based analysis and colon tracing, 2) detection of polyp candidates based on morphologic analysis on the segmented colon, 3) calculation of 3D pattern features of the polyp candidates, and 4) quadratic discriminant analysis for classification of the polyp candidates as polyps or non-polyps based on the pattern features.

2.2. Architecture of a 3D MTANN

To process 3D CTC volume data, we developed a 3D MTANN [14] by extending the structure of a 2D MTANN [15-17]. The architecture of the 3D MTANN is shown in Fig. 1. The 3D MTANN consists of a linear-output artificial neural network (ANN) model which is capable of operating on voxel data directly [18]. The 3D MTANN is trained with input CTC volumes and the corresponding "teaching" volumes for enhancement of polyps and suppression of non-polyps. The input to the 3D MTANN is the voxel values $I(x,y,z)$ in a sub-volume V_S extracted from an input volume. The output of the 3D MTANN is a continuous value, represented by

$$O(x,y,z) = NN\{I(x-i,y-j,z-k) \mid (i,j,k) \in V_S\}, \quad (1)$$

where $NN\{\bullet\}$ is the output of the linear-output ANN. The entire output volume is obtained by scanning of an input CTC volume with the 3D MTANN in 3D space.

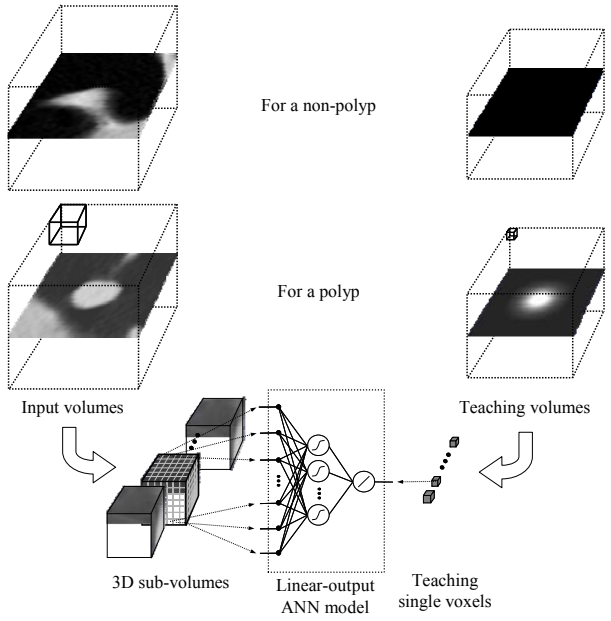

Fig. 1. Architecture and training of a single 3D MTANN consisting of a linear-output ANN model (i.e., the activation function of the output unit is a linear function instead of a sigmoid function) and a massive-subvolume training scheme. The input CTC volume including a polyp or a non-polyp is divided voxel by voxel into a large number of overlapping 3D sub-volumes. All voxel values in each of the sub-volumes are entered as input to the 3D MTANN, whereas a voxel value at each voxel from the teaching volume is used as the teaching value.

2.3. Training of a 3D MTANN

The training of a 3D MTANN is shown in Fig. 1. For enhancement of polyps and suppression of non-polyps, the teaching volume represents the "likelihood of being a polyp," which contains a 3D Gaussian distribution for a polyp or all zeros for a non-polyp, represented by

$$T(x,y,z) = \begin{cases} \dfrac{1}{\sqrt{2\pi}\sigma_T} \exp\left\{-\dfrac{(x^2+y^2+z^2)}{2\sigma_T^{\,2}}\right\} & \textit{for a polyp} \\ 0 & \textit{otherwise.} \end{cases}, \quad (2)$$

where σ_T is the standard deviation. The 3D MTANN is massively trained with a large number of sub-volumes extracted from input CTC volumes together with the corresponding voxels in the teaching volumes. The 3D MTANN is trained by a linear-output back-propagation algorithm [18]. After training, the 3D MTANN is expected to output a higher value for a polyp and a lower value for a non-polyp. For distinction between polyps and non-polyps, we developed a 3D scoring method based on the output volume of the trained 3D MTANN. A score for a given polyp candidate is defined as

$$S = \sum_{x,y,z \in V_E} f_G(\sigma;x,y,z) \times O(x,y,z), \quad (3)$$

where $f_G(.)$ is a 3D Gaussian weighting function with standard deviation σ,

$$f_G(\sigma_n;x,y,z) = \frac{1}{\sqrt{2\pi}\sigma_n} \exp\left\{-\frac{(x^2+y^2+z^2)}{2\sigma_n^{\,2}}\right\}, \quad (4)$$

and V_E is the volume used for evaluation.

2.4. A Mixture of Expert 3D MTANNs Architecture

To distinguish between polyps and various sources of FPs, we developed a "mixture of expert" 3D MTANNs . The architecture of the mixture of expert MTANNs is shown in Fig. 2. The mixture of expert MTANNs consisted of several 3D MTANNs. Each of the MTANNs was trained independently with a different type of FPs and common typical polyps. The 3D MTANNs were combined with a mixing ANN such that all major sources of FPs such as stool with bubbles, colonic walls, bulbous-shape folds, and solid stool could be removed. The scores of each expert 3D MTANN act as the features for distinguishing polyps from a specific type of non-polyp for which the expert 3D MTANN is trained. The output of the mixing ANN for the cth polyp candidate is represented by

$$M_c = NN\left[\{S_{n,c}\} \mid 1 \le n \le N\right] \quad (5)$$

where $NN(\bullet)$ is the output of the linear-output ANN model.

3. DATABASE OF CTC

Our testing database consists of CTC scans obtained from a multicenter clinical trial in which 15 leading medical institutions participated nationwide [12, 13]. Each patient was scanned in both supine and prone positions with a multi-detector-row CT system with collimations of 1.0-2.5 mm and reconstruction intervals of 1.0-2.5 mm. Each CT slice has a spatial resolution of 0.5-0.7 mm/pixel. A radiologist experienced in CTC (>1000 cases read) determined the locations of polyps with reference to colonoscopy reports. In the clinical trial, 155 patients had clinically significant polyps. Among them, about 45% of patients were false-negative (FN) interpretations. Those

patients had 114 "missed" polyps which were not detected by radiologists during their initial clinical reading. For testing our CAD scheme, 14 cases with 14 polyps/masses were randomly selected from the FN cases. Lesion sizes ranged from 6-35 mm, with an average of 10 mm.

Our training database consists of 200 CTC datasets obtained from 100 patients, each of whom was scanned in both supine and prone positions. Fourteen patients had 26 polyps, 12 of which were 5-9 mm and 14 were 10-25 mm in size. Each reconstructed CT section had a matrix size of 512 x 512 pixels, with an in-plane pixel size of 0.5-0.7 mm. All patients underwent "reference-standard" optical colonoscopy. We applied our initial polyp detection scheme to our CTC database. We used polyps and non-polyps (i.e., FP detections by our initial scheme) for training 3D MTANNs.

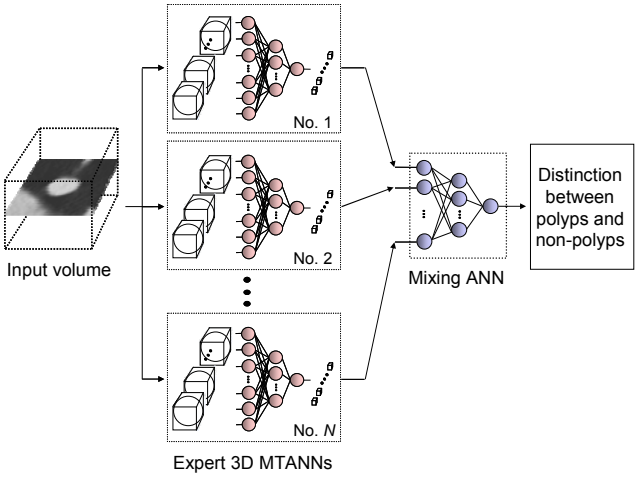

Fig. 2. A mixture of expert 3D MTANNs for distinguishing polyps from various types of FPs. The outputs of the expert 3D MTANNs are combined with a mixing ANN so that the mixture of expert 3D MTANNs can remove various types of non-polyps.

4. RESULTS

4.1. Performance of Our CAD Scheme

Our initial polyp-detection scheme yielded 43% (6/14) by-patient sensitivity with 5.6 (78/14) FPs per patient for the 14 "missed" polyp cases. To increase the sensitivity level, we changed the operating point for the performance of the initial polyp-detection scheme, and we obtained 71.4% (10/14) sensitivity with 18.9 (264/14) FPs per patient. We applied the trained expert 3D MTANNs for reduction of the FPs. The 3D MTANNs were able to remove 75% (197/264) of the FPs without removal of any TPs, as shown in Fig. 3. Thus, our CAD scheme achieved a by-patient sensitivity of 71% (10/14) with 4.8 (67/14) FPs per patient; therefore, our scheme has the potential to detect up to 71% of "missed" polyp cases. Some of the "missed" polyps by radiologists were very small or of the sessile type (these are major causes of human misses). Some sessile-type polyps are known to be histologically aggressive; therefore, detection of such polyps is critical clinically, but they are difficult to detect because of their uncommon morphology. Our CAD scheme detected these "difficult" polyps correctly. It should be noted that one polyp correctly detected by our CAD scheme had been missed in both CTC and "reference-standard" optical colonoscopy in the trial; thus, detection of this polyp may be considered "very difficult." Figure 4 illustrates a computer interface of CTC with our CAD marks.

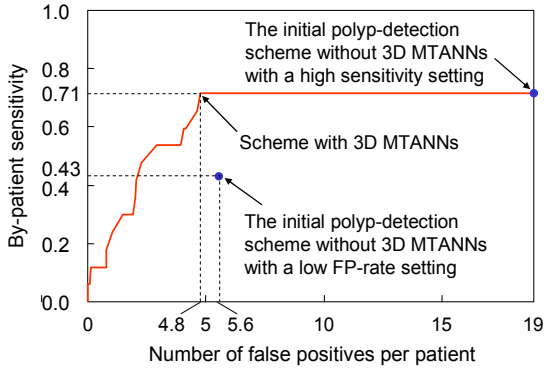

Fig. 3. Free-response receiver operating characteristic (FROC) curve for the performance of our CAD scheme consisting of an initial-polyp detection scheme and 3D MTANNs, indicating a substantial reduction of FPs by the 3D MTANNs. Our scheme achieved 71% by-patient sensitivity with 4.8 FPs/patient for 14 polyps "missed" by radiologists in the clinical trial.

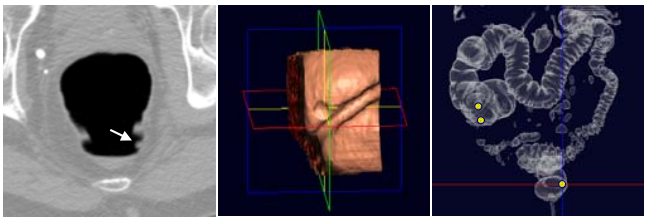

Fig. 4. A patient with a small (7 mm) sessile polyp that was "missed" in a clinical trial. (a) our CAD scheme incorporating 3D MTANNs correctly detected the polyp and pointed it by an arrow in an axial CTC image, (b) the polyp in the 3D endoluminal view, and (c) 3D volume rendering of the colon with three computer outputs indicated by yellow circles (one in the rectum is a true-positive detection and the other two are FP detections).

4.2. Analysis of False Positive Sources

The number of FPs with our CAD system was relatively small, but about five FPs per patient were still generated. We analyzed all FPs and categorized them into easy, moderate, and difficult. The easy case is defined as "it is obviously not a polyp" when viewed on 2D and/or 3D views. The moderate case would require interactive window/level adjustment and paging several times through the area. The difficult case, i.e., "pitfalls" with CAD, would require supine/prone comparison. Easy, moderate, and difficult cases accounted for 69% of all FPs, 18%, and 13%, respectively. The easy, moderate, and difficult cases included the ileocecal valve and respiratory motion, collapse and stool, and stool and hemorrhoid, respectively.

5. CONCLUSION

With our CAD scheme incorporating MTANNs, 71.4% of polyps "missed" by radiologists in the trial were detected correctly, with a reasonable number of FPs. Our CAD scheme would be useful for detecting "difficult" polyps which radiologists are likely to miss, thus potentially improving radiologists' sensitivity in detection of polyps in CTC.

6. ACKNOWLEDGEMENT

This work was supported by an RSNA Research Seed Grant, an American Cancer Society Illinois Division Research Grant, a University of Chicago Cancer Research Center Support Grant, and Grant Number R01CA120549 from the National Cancer Institute/National Institutes of Health.

7. REFERENCES

[1] P. J. Pickhardt, J. R. Choi, I. Hwang, J. A. Butler, M. L. Puckett, et al., "Computed tomographic virtual colonoscopy to screen for colorectal neoplasia in asymptomatic adults," *New England Journal of Medicine*, vol. 349, no. 23, pp. 2191-2200, 2003.

[2] P. B. Cotton, V. L. Durkalski, B. C. Pineau, Y. Y. Palesch, P. D. Mauldin, et al., "Computed tomographic colonography (virtual colonoscopy): a multicenter comparison with standard colonoscopy for detection of colorectal neoplasia," *JAMA*, vol. 291, no. 14, pp. 1713-9, 2004.

[3] A. H. Dachman, "Diagnostic performance of virtual colonoscopy," *Abdom. Imaging*, vol. 27, no. 3, pp. 260-267, 2002.

[4] H. M. Fenlon, D. P. Nunes, P. C. Schroy, 3rd, M. A. Barish, P. D. Clarke, et al., "A comparison of virtual and conventional colonoscopy for the detection of colorectal polyps," *New England Journal of Medicine*, vol. 341, no. 20, pp. 1496-1503, 1999.

[5] C. D. Johnson, W. S. Harmsen, L. A. Wilson, R. L. Maccarty, T. J. Welch, et al., "Prospective blinded evaluation of computed tomographic colonography for screen detection of colorectal polyps," *Gastroenterology*, vol. 125, no. 2, pp. 311-319, 2003.

[6] T. Doshi, D. Rusinak, R. A. Halvorsen, D. C. Rockey, K. Suzuki, et al., "CT Colonography: False-Negative Interpretations," *Radiology*, vol. 244, no. 1, pp. 165-73, 2007.

[7] H. Yoshida and J. Nappi, "Three-dimensional computer-aided diagnosis scheme for detection of colonic polyps," *IEEE Trans. Med. Imaging*, vol. 20, no. 12, pp. 1261-74, 2001.

[8] H. Yoshida, Y. Masutani, P. MacEneaney, D. T. Rubin, and A. H. Dachman, "Computerized detection of colonic polyps at CT colonography on the basis of volumetric features: pilot study," *Radiology*, vol. 222, no. 2, pp. 327-336, 2002.

[9] R. M. Summers, C. D. Johnson, L. M. Pusanik, J. D. Malley, A. M. Youssef, et al., "Automated polyp detection at CT colonography: feasibility assessment in a human population," *Radiology*, vol. 219, no. 1, pp. 51-59, 2001.

[10] A. K. Jerebko, R. M. Summers, J. D. Malley, M. Franaszek, and C. D. Johnson, "Computer-assisted detection of colonic polyps with CT colonography using neural networks and binary classification trees," *Med. Phys.*, vol. 30, no. 1, pp. 52-60, 2003.

[11] D. S. Paik, C. F. Beaulieu, G. D. Rubin, B. Acar, R. B. Jeffrey, Jr., et al., "Surface normal overlap: a computer-aided detection algorithm with application to colonic polyps and lung nodules in helical CT," *IEEE Trans. Med. Imaging*, vol. 23, no. 6, pp. 661-675, 2004.

[12] D. Rockey, E. Paulson, D. Rubin, R. Halvorsen, W. Thompson, et al., "CT colonography for detection of colon polyps and cancer," *Lancet*, vol. 365, no. 9469, pp. 1465-1466, 2005.

[13] D. C. Rockey, E. Paulson, D. Niedzwiecki, W. Davis, H. B. Bosworth, et al., "Analysis of air contrast barium enema, computed tomographic colonography, and colonoscopy: prospective comparison," *Lancet*, vol. 365, no. 9456, pp. 305-311, 2005.

[14] K. Suzuki, H. Yoshida, J. Nappi, and A. H. Dachman, "Massive-training artificial neural network (MTANN) for reduction of false positives in computer-aided detection of polyps: Suppression of rectal tubes," *Med. Phys.*, vol. 33, no. 10, pp. 3814-3824, 2006.

[15] K. Suzuki, F. Li, S. Sone, and K. Doi, "Computer-aided diagnostic scheme for distinction between benign and malignant nodules in thoracic low-dose CT by use of massive training artificial neural network," *IEEE Trans. Med. Imaging*, vol. 24, no. 9, pp. 1138-1150, 2005.

[16] K. Suzuki, S. G. Armato, F. Li, S. Sone, and K. Doi, "Massive training artificial neural network (MTANN) for reduction of false positives in computerized detection of lung nodules in low-dose CT," *Med. Phys.*, vol. 30, no. 7, pp. 1602-1617, 2003.

[17] K. Suzuki, H. Abe, H. MacMahon, and K. Doi, "Image-processing technique for suppressing ribs in chest radiographs by means of massive training artificial neural network (MTANN)," *IEEE Trans. Med. Imaging*, vol. 25, no. 4, pp. 406-416, 2006.

[18] K. Suzuki, I. Horiba, and N. Sugie, "Neural edge enhancer for supervised edge enhancement from noisy images," *IEEE Trans. Pattern Anal. Mach. Intell.*, vol. 25, no. 12, pp. 1582-1596, 2003.